

Cite this: *Lab Chip*, 2011, **11**, 3829

www.rsc.org/loc

PAPER

A microfluidic platform for pharmaceutical salt screening

Michael R. Thorson,^a Sachit Goyal,^a Benjamin R. Schudel,^a Charles F. Zukoski,^a Geoff G. Z. Zhang,^b Yuchuan Gong^{*b} and Paul J. A. Kenis^{*a}

Received 16th July 2011, Accepted 15th September 2011

DOI: 10.1039/c1lc20645a

We describe a microfluidic platform comprised of 48 wells to screen for pharmaceutical salts. Solutions of pharmaceutical parent compounds (PCs) and salt formers (SFs) are mixed on-chip in a combinatorial fashion in arrays of 87.5-nanolitre wells, which constitutes a drastic reduction of the volume of PC solution needed per condition screened compared to typical high throughput pharmaceutical screening approaches. Nucleation and growth of salt crystals is induced by diffusive and/or convective mixing of solutions containing, respectively, PCs and SFs in a variety of solvents. To enable long term experiments, solvent loss was minimized by reducing the thickness of the absorptive polymeric material, polydimethylsiloxane (PDMS), and by using solvent impermeable top and bottom layers. Additionally, well isolation was enhanced *via* the incorporation of pneumatic valves that are closed at rest. Brightfield and polarized light microscopy and Raman spectroscopy were used for on-chip analysis and crystal identification. Using a gold-coated glass substrate and minimizing the thickness of the PDMS control layer drastically improved the signal-to-noise ratio for Raman spectra. Two drugs, naproxen (acid) and ephedrine (base), were used for validation of the platform's ability to screen for salts. Each PC was mixed combinatorially with potential SFs in a variety of solvents. Crystals were visualized using brightfield polarized light microscopy. Subsequent on-chip analyses of the crystals with Raman spectroscopy identified four different naproxen salts and five different ephedrine salts.

Introduction

Salt screening and selection has been identified as the activity with the highest risk at the early stage of drug development.¹ A key challenge to identify salts of parent compounds (PCs) is screening an extensive number of salt formers (SFs) under a variety of crystallization conditions with limited material. Extensive screens are traditionally conducted at various conditions to identify salts with suitable properties for formulation development because many parameters influence crystallization of salts, including SF identity, PC to SF ratios, solvents employed, pH, and temperature.^{2,3} To carry out high-throughput screens, automated robotic systems have been developed, which improve efficiency and reduce turnaround time.⁴ However, these robotic tools typically require 0.5–1 gram of material to carry out a full screen (100–200 conditions at 10 mg ml⁻¹ in 500 μ l wells). In addition, crystallization is often jeopardized in such high-throughput methodology due to poor control of mixing. This study presents a microfluidic approach that addresses these challenges by enabling extensive salt screenings with reduced

sample requirement and much improved control over the crystallization processes.

Microscale approaches allow for screening of more extensive sets of conditions with sub-nanolitre volumes while affording better control over crystallization experiments. Over the last decade, advanced microscale platforms have been developed for a wide range of applications,^{5,6} including metering and mixing for crystallization.^{7–12} For example, Quake *et al.*, developed a highly integrated microfluidic platform to screen for crystallization of proteins using free interface diffusion (FID).⁹ Additionally, Ismagilov *et al.* and Laval *et al.* developed droplet based systems in which (sub) nanolitre-sized droplets of different composition are suspended in oil and screened for crystal formation.^{7,11} Ismagilov *et al.* also developed a well-based system, called “Slip-Chip”, in which, preloaded precipitants mix diffusively with protein solutions.¹³ Related, Myerson *et al.* developed a microscale platform for polymorph screening.¹⁴ While each of these approaches exhibit significant step forward in performing crystallization screens, they suffer from some of the following limitations: solvent compatibility, limited propensity for scale out, poor well isolation, limited portability due to required peripheral connections, and/or limited compatibility with analytical tools.

Here we report a microfluidic platform that overcomes some of the aforementioned limitations. This microfluidic platform is comprised of 48 wells. Each well is approximately 87.5 nL in

^aDepartment of Chemical & Biomolecular Engineering, University of Illinois at Urbana-Champaign, USA. E-mail: kenis@illinois.edu

^bMaterials Science, Global Pharmaceutical R & D, Abbott Laboratories, North Chicago, USA. E-mail: yuchuan.gong@abbott.com

volume (as opposed to 500 μl in a traditional approach) which constitutes over 5,000 fold reduction in material use. The reduction in volume enables salt screening even when less than one milligram of the parent compound is available. For example, to screen 200 conditions at 10 mg ml^{-1} , our microfluidic chip would require only 175 μg of PC. PCs in various solvents and at various concentrations are mixed in a combinatorial fashion with SF solutions. The diffusive mixing on-chip enables the solutions on-chip to slowly reach their final supersaturation levels (~ 20 min). These chips are designed such that solvent absorption and evaporation are minimized, which allows for use of solvents commonly utilized for salt screening. In addition, Actuate-to-Open valves (AtO) improve the long term well-to-well isolation because they completely seal the wells at rest.¹⁵ Thus solvents are contained as necessary for long term experiments. The chips were designed to enable on-chip analysis of crystals with Raman spectroscopy for identification of solid forms (polymorphism, salt identity). We validated the functionality of the microfluidic chip using two model systems, naproxen and ephedrine.

Materials and methods

The crystallization platform is comprised of a thin multilayer polydimethylsiloxane (PDMS, General Electric RTV 650 Part A/B) chip fabricated using standard multilayer soft lithographic procedures reported previously^{9,16} with some modifications. The control layer thickness was reduced to 70 μm by spin coating the PDMS (5 : 1 A : B) at 1300 rpm. Next, the control layer was bonded to a PDMS frame (a 2.5" square PDMS slab with a 2" by 1" window in the center) *via* heating at 60 $^{\circ}\text{C}$ for 30 min, to provide rigidity and allow for transfer of the control layer. Once bonded, two millilitre of hexane was poured onto the control layer, which caused the thin PDMS control layer to swell and peel off the silicon wafer. Next, the control layer was rinsed with water to remove residual hexane, dried, aligned and placed on the fluid layer, and heated at 60 $^{\circ}\text{C}$ for 30 min for bonding. Crystal Clear Tape (Hampton HR4-511), which is impermeable to solvents, was adhered to top of the combined control and fluid layers. The glass substrate on which the assembled fluid and control layers are placed was coated with thin layers of chromium and gold. Pre-cleaned microscope slides (Fischer Scientific 12-550-A3) were coated with a 20 nm layer of chromium and on top of the chromium, a 200 nm layer of gold using an E-beam evaporation system (Temescal six pocket E-Beam Evaporation System).

All PCs and SFs were obtained from Sigma-Aldrich and used as provided. The following procedure was used for the preparation of naproxen solutions. Fifty milligrams of naproxen each was dispensed into four vials and methanol, ethanol, isopropanol, and water were added to the respective vials until naproxen completely dissolved while the vials were sonicated (Branson 2510). Next an additional 100 μl of solvent was added to each vial, thereby ensuring that each naproxen solution was below its solubility in the solvent used. The resultant naproxen concentrations in ethanol, methanol, isopropanol, and water were 21 mg ml^{-1} , 27 mg ml^{-1} , 26 mg ml^{-1} , and 0.05 mg ml^{-1} , respectively. SF solutions of sodium hydroxide, potassium hydroxide, pyridine and arginine were prepared in methanol and isopropanol. The SF concentrations were formulated such that

the SF:PC molar ratios when mixed on-chip were 1.2 : 1 for naproxen solution with the highest solubility, here the methanol solution for all four cases.

The procedure for preparing ephedrine solutions and SF solutions was similar to the procedure described above for naproxen except for the identity of the solvents and the actual concentrations used. Ephedrine was dissolved in one solvent, methanol, at a concentration of 2.2 grams per millilitre of solvent. Six acid solutions in methanol were prepared, based on hydrochloric, sulfuric, methane sulfonic, ethane sulfonic, nitric and phosphoric acids, such that the resulting molar ratio of each SF and ephedrine combination when mixed on-chip was 1.2 : 1.

All solutions used on-chip were introduced by first pipetting 1–2 μl droplets at the inlet ports, then, pulling the fluid into the chip *via* actuation of the appropriate valve sets and applying gentle suction at the appropriate fluid outlets. Once filled, the PC and SF solutions were mixed diffusively for 20 min as discussed later. After the solutions fully mixed, all peripheral connections (tubing for pneumatic control) were disconnected and the chip was sealed with Crystal Clear Tape (Hampton Research) to prevent solvent evaporation.

Throughout the mixing period and for the following 2–24 h after mixing, the wells were periodically monitored visually for solid formation on an automated computer controlled imaging upright optical microscope (Leica Z16 APO) equipped with a macro lens (Leica 10447176), a digital camera (Leica DFC280), and a motorized X-Y stage (Semprex KL66). Photo images of each well were acquired every 30 min by moving the automated motorized stage in a sequential fashion between wells using Image Pro Plus (Media Cybernetics).

Within two hours of nucleation, the crystallinity of the solid forms was verified using birefringence (chips without the gold coating). When a gold coating was applied to the glass slide, Raman spectroscopy (Renishaw mircoPL/Raman microscope) was used to analyze and identify the different solid forms. The Raman setup is based on an upright microscope (Leica DM2500M) equipped with a 785 nm excitation source. Using a 5 \times objective in brightfield mode, individual wells were centered under the objective. By moving to higher magnification (20 \times or 50 \times), the Raman light source was focused (spot size $\sim 5 \mu\text{m}$) on individual crystals to obtain Raman spectra in the range of 350–1750 cm^{-1} .

To obtain reference Raman spectra of the salts of ephedrine, the salts were crystallized off-chip in glass vials. Each vial was filled with ephedrine solutions in methanol (2.2 g ml^{-1} , 13.3 mmol ml^{-1}). The following SF/methanol solutions (13.3 mmol ml^{-1}) were added to the ephedrine solution to make the final solutions 20% molar excess with respect to ephedrine: hydrochloric acid, sulfuric acid, methane sulfonic acid, ethane sulfonic acid, nitric acid and phosphoric acid. The vials were sonicated (Branson 2510) and, subsequently, left open to atmosphere to induce crystallization. Crystals were harvested from the respective vials and analyzed under the Raman microscope (Renishaw mircoPL). The Raman spectra obtained were used to identify the ephedrine salts formed on chip in combination with the spectra obtained from crystals off-chip to identify the solids formed on-chip. Raman spectra of the salts of naproxen are available in the literature.^{17–19}

We simulated diffusive mixing within the parent compound (PC) and SF chambers using a 3D finite elements solver,

FEMLAB 3.5a (Comsol, Stockholm, Sweden). The dimensions of the PC and SF chambers in this model are identical to the dimensions of the actual chip: All chambers were 50 μm tall; the PC chamber was 1.25 mm by 1.0 mm and the SF chamber was 0.5 mm by 1.0 mm. The 1.0 mm sides of the adjacent PC and SF chambers were separated by a 50 μm wide wall which has embedded a 25 μm tall and 0.6 mm wide mixing valve. All external and internal boundaries were classified as “insulation” and “continuity” respectively. The mesh size was “extra fine”.

The initial concentration of PC in the PC chamber was 20 mg ml^{-1} , the initial concentration of succinic acid in the SF chamber was 47 mg ml^{-1} and the concentration of all solutions in the mixing chamber was assumed to be zero. The model was run for 2000 s (~ 33 min) at 100 s intervals. The following diffusivities were used: methanol in water: $1.28 \times 10^{-5} \text{ cm}^2 \text{ s}^{-1}$, water in methanol: $1.28 \times 10^{-5} \text{ cm}^2 \text{ s}^{-1}$, SF (succinic acid) in ethanol: $1 \times 10^{-5} \text{ cm}^2 \text{ s}^{-1}$, and candidate drug (acetaminophen) in water $4.25 \times 10^{-6} \text{ cm}^2/\text{s}$.^{20,21} The solutions were assumed to be dilute and the diffusion coefficients were assumed to be independent of concentration. This approximation is reasonable because the

model will depend more on the diffusing species rather than concentrations.

Results and discussion

Design and operation of microfluidic crystallization platform

The microfluidic crystallization platforms developed here will assist in the screening of different salts of a given pharmaceutical compound. The desired platform needs to screen many conditions while consuming minimal amounts of material and be compatible with an external analysis method such as microscopy and/or Raman spectroscopy.

Chip design. The microfluidic platform is fabricated and assembled using multilayer soft lithography procedures¹⁶ with some modifications (see Materials and methods). The resulting multilayer structure comprised of fluid and control layers is placed on a glass slide (Fig. 1). The microfluidic network is designed such that solutions of a PC in up to four different

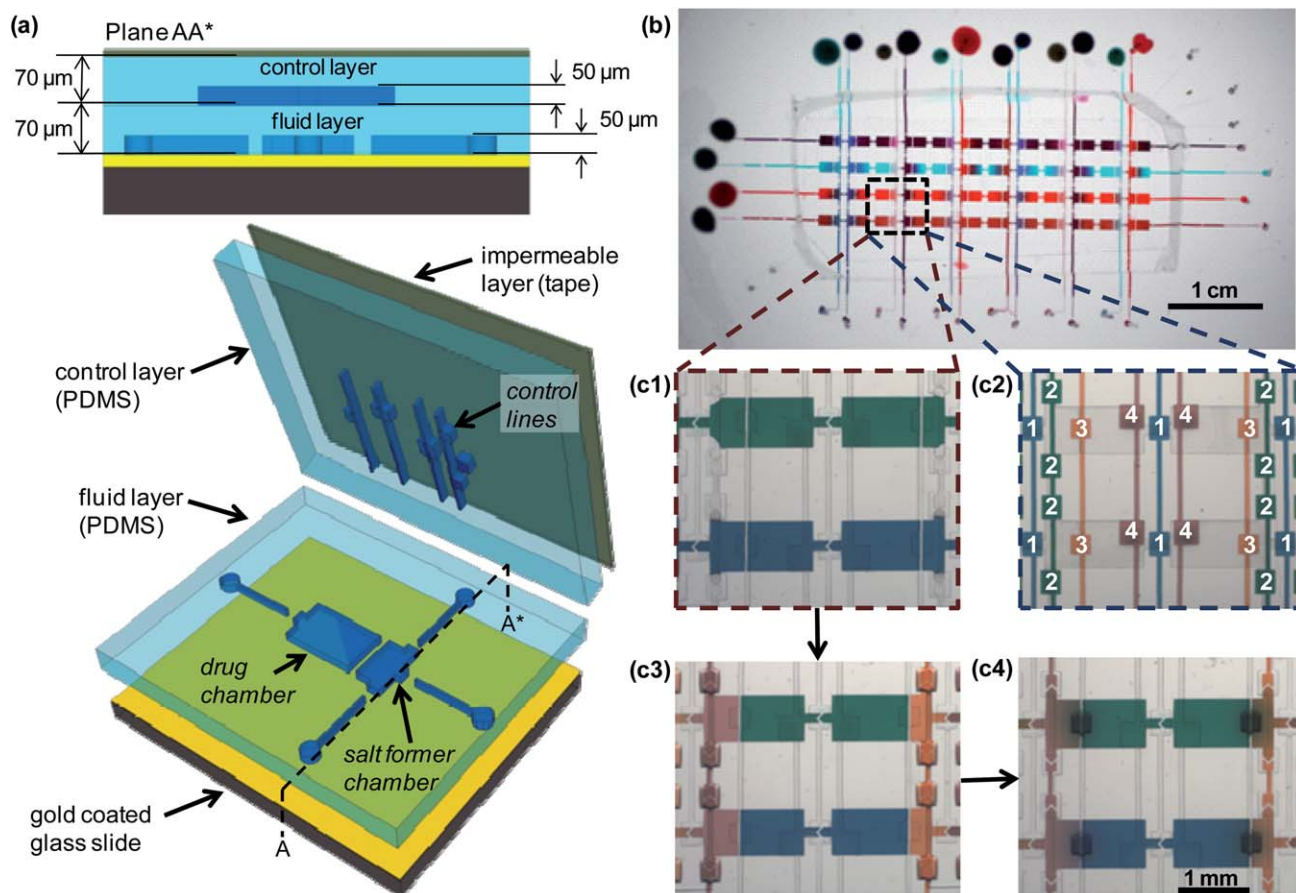


Fig. 1 (a) Schematics of the layered design of a single microfluidic crystallization well, comprised of a fluid layer with chambers for SF and PC solutions, and a control layer with the pneumatic control lines and valves. This assembly is sandwiched between an impermeable layer and a glass slide to provide rigidity and reduce solvent loss. The gold coating on the glass slide reduces noise for on-chip analysis of the crystals with Raman spectroscopy. (b) An optical micrograph of a microfluidic crystallization screening chip comprised of a 4×12 array of wells filled with food dye solutions highlights the chip's combinatorial mixing capabilities. (c) Enlarged view of a 2×2 set of wells to visualize the filling and mixing process. First the PC solution is introduced horizontally (valves 1 and 3 actuated) and locked up in the PC chambers (c1). Then SF solutions are introduced vertically (valves 2 are actuated) and locked up in their respective chambers (c2). Then the valves between adjacent PC and SF chambers (valves 3) are opened to allow the solutions to mix (c3). Back-and-forth actuation of valves 4 can be used to speed up the slow diffusive mixing process.

solvents (or at up to four different concentrations in the same solvent) are mixed in a combinatorial fashion with up to 12 SF solutions resulting in 48 unique conditions. Each condition (or “well”) requires a volume of only 62.5 nL for PC, so at typical PC concentrations of 20–200 mg ml⁻¹, each condition screened consumes only 1.25–12.5 µg of PC. Each “well” is comprised of an isolated chamber for a PC solution and an isolated chamber for a SF solution (Fig. 1a). The dimensions of the different chambers are optimized to minimize the volume used per well. The volume of the SF chamber is 2.5 times smaller relative to the volume of the PC chamber to minimize dilution effects. The solubility of SF and the need to mix a certain amount of SF with PC prohibit further reduction of the volume of the SF chamber. Additionally, the wells need to be designed such that diffusional mixing is achieved fast enough for a high-throughput application (*i.e.*, in less than 30 min) and slow enough to prevent massive precipitation at the onset of mixing. The one-dimensional length to mix within a time t can be estimated using Fick’s law, $x = 2(Dt)^{1/2}$, where x is the combined length of the long side of the SF and the PC chambers, and D is the diffusivity of the diffusing species, here approximated from the diffusivity of acetaminophen in water, 4.25×10^{-6} cm²/s.²⁰ For a mixing time of 20 min, x is about 1 mm, so we ensured that the total length of the SF and PC chambers in the microfluidic chip was roughly 1 mm.

Chip operation. The chambers and various feed lines are isolated by valves that are closed when at rest (Fig. 1a). These valves open upon applying a negative pressure to the control lines.¹⁵ Four sets of these normally closed valves are incorporated in the control layer: Valves for filling the SF chambers (the set labelled “1” in Fig. 1c2), valves for filling the PC chambers (set 2), valves that enable diffusive mixing between the PC and SF (set 3), and valves that can speed up (*via* added convection), if needed, the diffusive mixing through repeated actuation (set 4). Using a pipette, 1–2 µl droplets of the different PC and SF solutions are placed over the inlets of the rows and columns, respectively (Fig. 1b). Then, the PC solutions are introduced horizontally by actuation of valve set 1 (Fig. 1c1), and applying gentle suction at the outlet of the row being filled. After closing this valve set, and thereby locking up the PC solutions in the PC chambers, the SF chambers are purged with a methanol solution and subsequently, the SF solutions are introduced vertically by actuation of valve set 2 (Fig. 1c3) in combination with gentle suction at the corresponding outlet. After closing valve set 2, and thereby locking up the SF solutions in their corresponding chambers, diffusional mixing of combinatorial combinations of PC solutions and SF solutions confined in adjacent chambers is induced by opening valve set 3 for about 20 min (Fig. 1c4). The mixing time can be reduced from 20 to 5 min by repeated actuation of valve set 4. After mixing, all pneumatic lines can be detached from the chip because all valves are closed when not actuated, thus isolating all individual experiments in each of the wells from each other.

Solvent compatibility. Solvent absorption by PDMS as well as solvent loss by evaporation could potentially limit the applicability of these chips for PC crystallization screening.²² To address these issues, we minimized the thickness of the PDMS fluid and control layers, and we used solvent impermeable top and bottom layers (Fig. 1a). As already stated above, the fluid layer is placed

on a glass slide, thus preventing solvent evaporation through the bottom. Crystal Clear tape is applied to the top of the chip, providing a solvent impermeable layer over the PDMS surface. In addition, the same impermeable tape is used to close all of the inlet and outlet ports immediately after mixing. Reducing the thickness of the PDMS layers from the typical several millimetres to ~140 µm, limited the absorption of water, methanol, and ethanol to 0.75%, 4.5% and 22%, respectively, of the total on-chip volume of all chambers and feed lines while taking into account each solvent’s partitioning coefficient into PDMS.¹⁷ These solvent absorption percentages are a factor of 14 smaller than those for a 2 mm thick PDMS chip. Reducing PDMS layer thickness and application of solvent impermeable layers on the top and bottom of the chip reduced solvent loss to the extent that the chips can be filled with methanol, ethanol, and isopropanol; solvents that are typically used in PC salt screening.^{23–25} While we limited this study to alcohols, we conjecture that a much broader range of solvents typically used with pharmaceutical industry (ketones, ethers, acetates) will also be compatible. Lee *et al.*, ranked the compatibility of various solvents with PDMS devices. Of the 38 solvents tested, 1-propanol, ethanol, and methanol were ranked 21, 24, and 28, respectively.²² We believe this platform will be compatible with many solvents in the range of ~19 to 38 by Lee, *et al.* (*e.g.*, ethyl acetate, dimethylformamide, dimethyl sulfoxide, propylene carbonate, and ethylene glycol).²² Further solvent compatibility would require integration of polymeric coatings²⁶ (*e.g.* CYTOP) to further reduce the PDMS/solvent interaction or use of alternative polymers²⁷ (*i.e.*, SIFEL). The less “compatible” a solvent is, the more a solvent will absorb into the PDMS (even when reduced), which will affect the concentration of the PC within the well. To accurately analyze wells with less “compatible” solvents, solvent absorption will have to be accurately analyzed. However, most solvents do not react with PDMS²² and as a result, when the PDMS becomes saturated with the solvent, the wells will not lose more solvent and the wells should not dry out for several days. After combinatorial mixing of the PC and SF solutions, various analysis methods, such as brightfield microscopy and Raman spectroscopy, are used for visualization and identification of the solid forms in each well (See below).

Simulation of FID mixing on-chip

We modeled the time dependent diffusion of the PC and SF species, as well as their respective solvents (1) to estimate the time required for the PC and SF solutions to fully mix; and (2) to correlate local concentrations of all species, obtained from the time-dependent concentration profiles, with the onset of crystal nucleation and growth. The latter information will aid in identifying suitable crystallization conditions for scale-up. We used finite-element-method modelling (Comsol) to simulate in 3D the time-dependent diffusional mixing of the PC, SF, and their respective solvents in the PC and SF chambers upon opening the mixing valve (valve 3, Fig. 1c3), which opens to 50% of the chamber height. From the modelling data we determined the time for a species to reach a ‘fully mixed’ state (defined as the time at which the highest and lowest local concentrations of a species inside the chambers differ by less than 10%) to be 16 and 11 min for the PC and SF, respectively, and 8 min for both

solvents. Using dyed solutions we confirmed experimentally that reaching a visually completely mixed state (homogeneous color) indeed takes less than 20 min. Based on these results, the valves between adjacent PC and combination chambers were left open for 20 min in all crystallization screens to ensure complete mixing. Fig. 2 shows concentration profiles of the four species for different times between 0 and 2000 s (~33 min) along the centerline connecting the two chambers at a height of 25% of the channel height. The apparent tiny peak in concentration at the location of the valve edge seen in all profiles at time = 0 s is an artifact resulting from mesh size. From the profiles, it is clear that most of the mixing takes place in the first 300 s (5 min). This also is in agreement with our experimental observations that most nucleation events are observed within the first few minutes after mixing and in close proximity of the mixing valve. In comparison, conventional approaches such as robotically filled micro-well plates mix PC and salt solutions nearly instantaneously, thereby increasing the supersaturation level too quickly and decreasing the likelihood of salt crystallization. Similarly, droplet based microfluidic crystallization techniques mix much faster due to convection within the droplet.¹¹ A more detailed study of the influence of supersaturation and concentration levels on on-chip crystallization (both on-chip and off-chip) will be included in a forthcoming paper.²⁸

The simulation results provide insight not only regarding the time it takes to reach a fully mixed solution, but also on the local

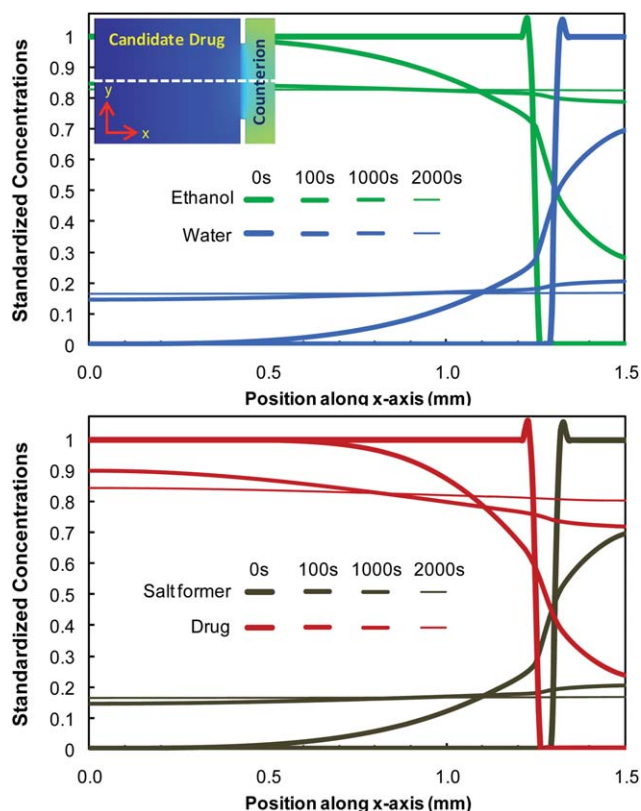


Fig. 2 Results from a 3D Finite Element Method simulation (Comsol) of on-chip mixing over 2000 s between the SF and PC solutions. The graphs show the evolution of concentration gradients of both solvents (top) and the PC & the SF (bottom) along the centerline (white dotted line in inset) at 25% of the height of the channel.

concentration resulting in the solid formation of a PC or a certain PC - SF combination. After recording the exact time and location of a crystallization event in an experiment, we can identify the corresponding local concentrations of the PC, SF and the solvents using data from the simulation. This information can then be used to setup subsequent experiments and identify potential conditions for scaling up the salt later in the drug development process. Further, in depth analyses of the results from screening experiments, including direct comparison to off-chip results, and corresponding simulations can provide insight into the crystallization characteristics, both thermodynamically and kinetically, of a PC or PC salt, which will be the topic of a forthcoming paper.

Drug salt screens

Naproxen (an acid) and ephedrine (a base), two commercially available drugs, were used for validation of on-chip salt screening. Each of these two PCs were mixed combinatorially with several SFs in 48-well chips to screen for possible crystalline salts. The wells were monitored for crystal formation using a bright field microscope.

Naproxen salt screening. Naproxen was chosen as a model compound for the demonstration of the chip's screening capabilities based on its known propensity for salt formation.¹⁹ Naproxen was dissolved in ethanol, methanol, isopropanol, and water at different concentrations (see Section 2). The SF solutions were comprised of NaOH, KOH, Pyridine, or Arginine dissolved in methanol or isopropanol. These solutions were prepared such that the molar ratio of SF to PC in the resulting combinatorial mixtures was 1.2 to 1. Fig. 3 shows an optical micrograph of a whole 48-well chip. In some wells, crystallization started within seconds following mixing of adjacent PC and SF solutions. Naproxen crystallized with KOH in 44% of the wells, with NaOH in 56% of the wells, with arginine in 25% of the wells, and with pyridine in 50% of the wells. The enlarged views in Fig. 3 show typical examples of the crystals formed for each of these salts. Further analyses of the different solid forms are discussed below.

Ephedrine salt screening. We also used ephedrine to validate the chip with a basic drug and various acids as the SFs.^{29,30} Ephedrine, dissolved in methanol at four different concentrations (see Materials and methods), was mixed in a combinatorial fashion with methanol solutions of six acids: hydrochloric, sulfuric, methane sulfonic, ethane sulfonic, nitric, and phosphoric acids (Fig. 4). Crystals were obtained in the wells of all acids, except nitric acid. Ephedrine crystallized with hydrochloric acid in 25% of the wells, while it crystallized in all wells with sulfuric, methane sulfonic, ethane sulfonic, and phosphoric acids. The enlarged views of individual wells in Fig. 4 show typical examples of the crystals formed for each of these salts.

On-chip analysis: birefringence and Raman spectroscopy

The presence and crystallinity as well as the size and shape of a solid form in a given microfluidic well can typically be determined using brightfield microscopy (see for example the enlarged

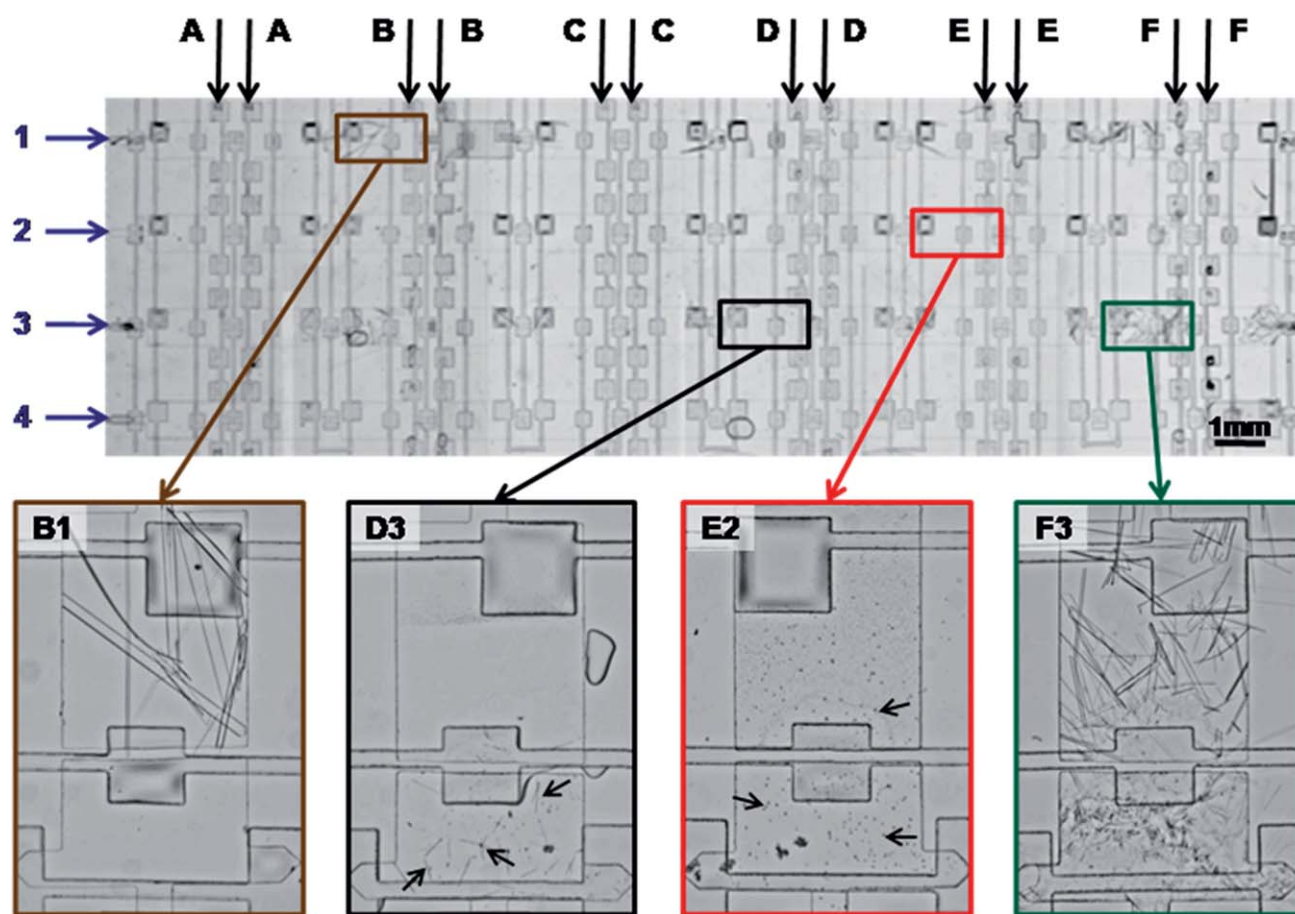


Fig. 3 On-chip screen of salt solid forms of Naproxen. Rows 1, 2, 3, and 4 are filled with Naproxen in ethanol, isopropanol, methanol and water, respectively. Columns A, B, C, D, E and F are filled with either methanol or isopropanol solutions of the following SFs: sodium hydroxide, sodium hydroxide, potassium hydroxide, arginine, pyridine, and potassium hydroxide, respectively. Sodium, arginine, pyridine and potassium salt crystals of Naproxen are visible in the enlarged views (rotated 90° clockwise with respect to the view of the whole chip).

views B1, D3, and F3 in Fig. 3). For some wells, however, it is unclear whether the solid form is crystalline or amorphous (*e.g.*, enlarged view E2 in Fig. 3). Viewing the individual wells with crossed polarized filters typically overcomes this issue because most crystals exhibit birefringence (see enlarged views in Fig. 4). However, microscopic approaches do not reveal the chemical identity of a crystal. It is particularly important to determine the chemical identity of the crystals observed on-chip because crystals of the free PC and/or the free SF may form in addition to, or instead of, crystals of the intended salts.

Analytical techniques such as IR spectroscopy, Raman spectroscopy, and X-ray analysis can be used for unequivocal identification of the crystalline material formed in a crystallization experiment. In this work, we used Raman spectroscopy for on-chip analysis of the crystals residing in the different wells (Fig. 5 and Fig. 6). The microfluidic crystallization screening chips were made compatible with Raman spectroscopy by reducing the thickness of the PDMS layers to less than 150 μm and by introducing a reflective gold coating on the glass substrate of the chip (see Fig. 1a) to reduce or eliminate noise from the PDMS and glass, respectively. Successively, multiple individual crystals are located and centered in brightfield mode at up to 50x magnification, and then, Raman spectra of these individual

crystals are obtained. Fig. 5 shows typical Raman spectra of four Naproxen salt crystals imaged on chip after performing the Naproxen salt screen described earlier. The enlarged view of the 700–850 cm^{-1} region shows unique peaks that identify each of the salts, which compare well to previously reported spectra for these salts.^{17–19} Fig. 6 shows Raman spectra for crystals of five different ephedrine salts. Since no literature data on ephedrine salts was available, we compare Raman spectra of crystals obtained on-chip and off-chip. The enlarged view of the 725–1075 cm^{-1} region shows both unique peaks for each of the salts and agreement between the spectra from the on-chip and off-chip grown crystals. In summary, the chip was able to screen for salts of both a basic and an acidic drug, and the formed salts could be distinguished from each other *via* on-chip analysis using Raman Spectroscopy.

Conclusions

We developed a microfluidic platform for screening and analysis of pharmaceutical salts. The platform mixes PC solutions combinatorially with SF solutions, to create an array of 4×12 unique conditions. The 87.5-nl wells of microfluidic chips are significantly smaller than the wells that are typically used in

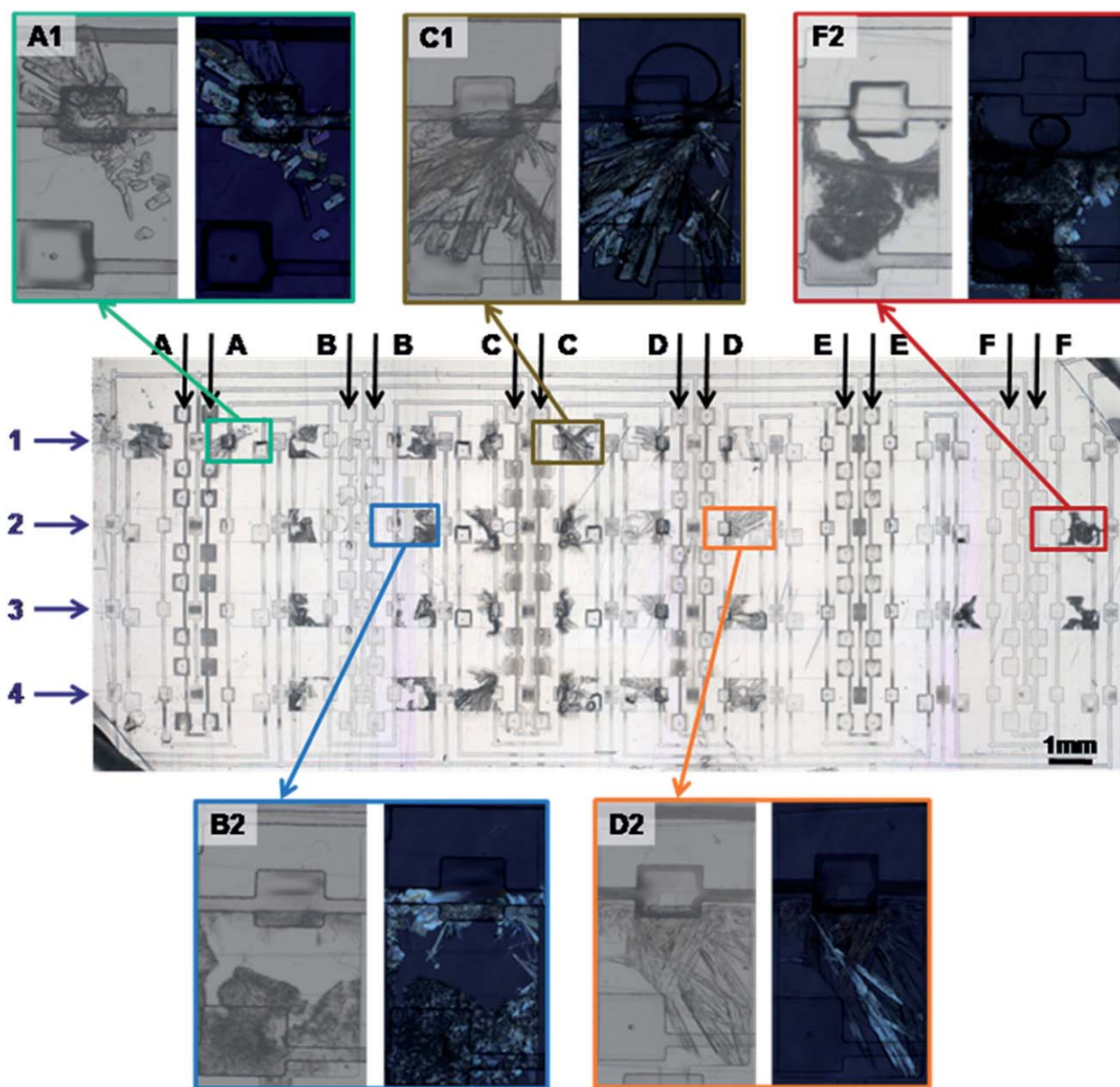


Fig. 4 On-chip screen of salt solid forms of ephedrine. Rows 1, 2, 3 and 4 are filled with Ephedrine in methanol. Columns A, B, C, D, E and F are filled with the following SFs in methanol: hydrochloric, sulfuric, methane sulfonic, ethane sulfonic, nitric, and phosphoric acids, respectively. Brightfield and birefringence images of hydrochloride, mesylate, dihydrogen phosphate, bisulfate, and esylate salt crystals of ephedrine are visible in the enlarged views (rotated 90° clockwise with respect to the view of the whole chip).

traditional robotic systems for pharmaceutical salt screenings. Mixing by free interface diffusion of the PC and SF solutions induces high local supersaturation which enhances the chance of crystallization. Reduction of the PDMS layer thickness and use of impermeable capping layers minimizes solvent loss, thus enabling the application of organic solvents such as methanol, ethanol, and isopropanol, which are typically used in pharmaceutical salt screening. Incorporation of valves that are closed in rest improved solvent containment, which is convenient for long-term experiments, as well as device portability, which is convenient for on-chip analysis after crystals have formed. The simplicity of the chip enables immediate application in laboratories because its use only requires pipettes and a low vacuum source.

Using naproxen and ephedrine, we have demonstrated that this microfluidic chip can be employed to screen for and identify multiple crystalline salt forms of PCs using only a limited amount of material. The solid forms can be analyzed on-chip, without harvesting. Information regarding shape and size is obtained using optical microscopy while information regarding the identity of the salt is obtained with Raman spectroscopy. These capabilities are especially beneficial in the early stage of drug development when the availability of compounds is limited.

We used modelling to predict diffusional mixing rates and concentration profiles of the PC, SF and the solvents to aid the design of the microfluidic chips. Furthermore, experimentally observed crystallization events can be combined with information from these modelled concentration profiles to identify the

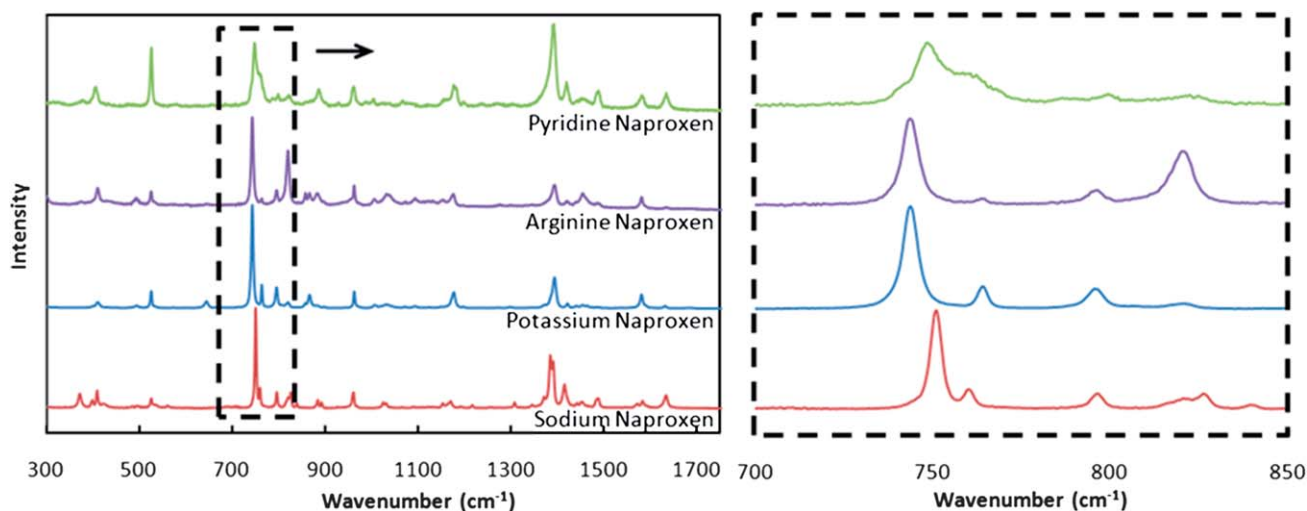


Fig. 5 On-chip analysis of various naproxen salt crystals using Raman spectroscopy. Magnified views of the 700–850 cm^{-1} range are provided to highlight the spectral differences between the different salts.

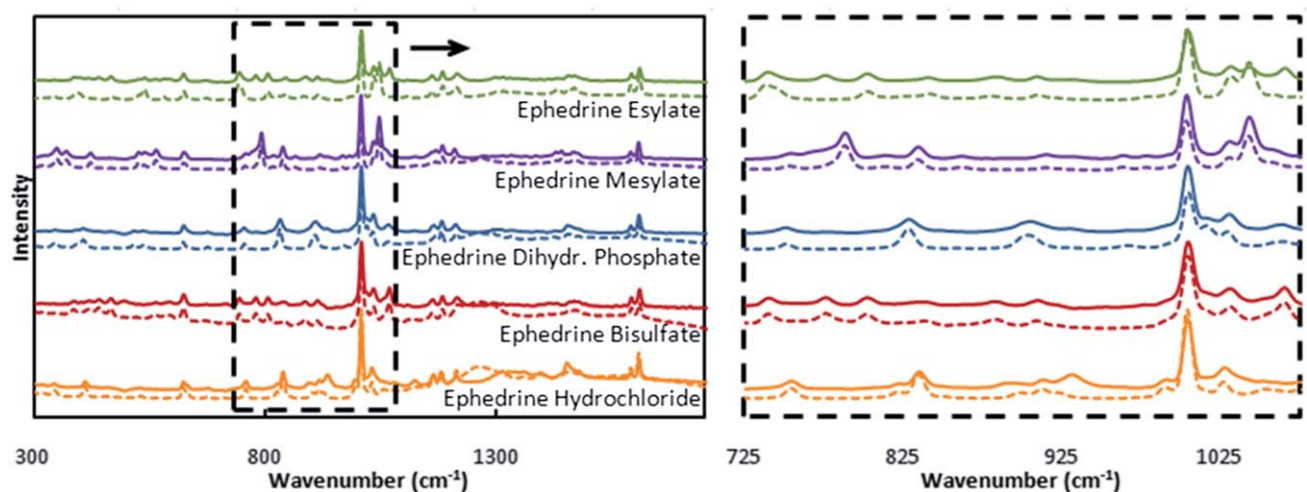


Fig. 6 Analysis of five ephedrine salts formed on-chip (solid lines) and off-chip (dashed lines) using Raman spectroscopy. Magnified views of the 725–1075 cm^{-1} range are provided to highlight the spectral differences between the different salts.

condition associated with the onset of crystallization. This condition can be replicated later on in the drug development process in scale up.

The microfluidic platform reported here can also find its application in salt screening using evaporation and/or antisolvent modes. Other high throughput crystallization applications include the screening for crystal habit, polymorphs or co-crystals covering wide ranges of conditions while using minimal amounts of material. Furthermore, modifications to the microfluidic chips, specifically the mixing zone and chamber geometries, would change the rate of supersaturation, thereby influencing crystallization events. In summary, with simple modifications, this platform could be used to study the nucleation, polymorphism and crystal habit of drugs and other compounds.

Acknowledgements

We would like to thank Abbott Laboratories for financial support. Part of this work made use of the facilities in the Micro-

& Nanotechnology Laboratory as well as the Frederick Seitz Materials Research Laboratory Central Facilities at University of Illinois at Urbana-Champaign, which are partially supported by the U.S. Department of Energy under grants DE-FG02-07ER46453 and DE-FG02-07ER46471.

Notes and references

- 1 C. Pingyun and D. Igo, *Drug Dev. Discovery*, 2011, **11**, 38–40.
- 2 D. L. Chen and R. F. Ismagilov, *Curr. Opin. Chem. Biol.*, 2006, **10**, 226–231.
- 3 J. R. Luft, J. Wolfley and I. Jurisica, *et al.*, *J. Cryst. Growth*, 2001, **232**, 591–595.
- 4 P. Desrosiers, *Modern Drug Discovery*, 2004, 40–43.
- 5 T. M. Squires and S. R. Quake, *Rev. Mod. Phys.*, 2005, **77**, 977–1026.
- 6 H. A. Stone, A. D. Stroock and A. Ajdari, *Annu. Rev. Fluid Mech.*, 2004, **36**, 381–411.
- 7 P. Laval, N. Lisai and J. B. Salmon, *et al.*, *Lab Chip*, 2007, **7**, 829–834.
- 8 P. Laval, J. B. Salmon and M. Joanicot, *J. Cryst. Growth*, 2007, **303**, 622–628.
- 9 C. L. Hansen, E. Skordalakes and J. M. Berger, *et al.*, *Proc. Natl. Acad. Sci. U. S. A.*, 2002, **99**, 16531–16536.

- 10 D. L. L. Chen, L. Li and S. Reyes, *et al.*, *Langmuir*, 2007, **23**, 2255–2260.
- 11 B. Zheng, L. S. Roach and R. F. Ismagilov, *J. Am. Chem. Soc.*, 2003, **125**, 11170–11171.
- 12 T. Thorsen, S. J. Maerkl and S. R. Quake, *Science*, 2002, **298**, 580–584.
- 13 L. Li, W. Du and R. Ismagilov, *J. Am. Chem. Soc.*, 2010, **132**, 106–111.
- 14 A. Y. Lee, L. Sung and S. Dette, *et al.*, *J. Am. Chem. Soc.*, 2005, **127**, 14982–14983.
- 15 B. R. Schudel, C. J. Choi and B. T. Cunningham, *et al.*, *Lab Chip*, 2009, **9**, 1676–1680.
- 16 M. A. Unger, H. P. Chou and T. Thorsen, *et al.*, *Science*, 2000, **288**, 113–116.
- 17 M. Varghek, T. B. Freedman and E. Lee, *et al.*, *Chem. Phys. Lett.*, 1998, **287**, 359–364.
- 18 A. Jubert, M. L. Legarto and N. E. Massa, *et al.*, *J. Mol. Struct.*, 2006, **783**, 34–51.
- 19 E. D. Carlson, P. Cong and W. H. Chandler, *et al.*, *PharmaChem*, 2003, **2**, 10–15.
- 20 H. Razmi and M. Harasi, *J. Iranian Chem. Soc.*, 2007, **5**, 296–305.
- 21 R. H. Perry and D. Green, *Perry's Chemical Engineer's Handbook*, McGraw-Hill, 2003.
- 22 J. N. Lee, C. Park and G. M. Whitesides, *Anal. Chem.*, 2003, **75**, 6544–6554.
- 23 J. F. Remenar, J. M. MacPhee and B. K. Larson, *et al.*, *Org. Process Res. Dev.*, 2003, **7**, 990–996.
- 24 E. Ware and D. R. Lu, *Pharm. Res.*, 2004, **21**, 177–184.
- 25 C. R. Gardner, O. Almarsson and H. Chen, *et al.*, *Comput. Chem. Eng.*, 2004, **28**, 943–953.
- 26 C.-S. Lee, S.-H. Lee and S.-S. Park, *et al.*, *Biosens. Bioelectron.*, 2003, **18**, 437–444.
- 27 G. Maltezos, E. Garcia and G. Hanrahan, *et al.*, *Lab Chip*, 2007, **7**, 1209–1211.
- 28 M. R. Thorson, S. Goyal, G. G. Z. Zhang, *et al.*, submitted.
- 29 N. B. Simon, A. C. Edwin and J. D. Roger, *et al.*, *J. Pharm. Sci.*, 2007, **96**, 1053–1068.
- 30 E. A. Collier, R. J. Davey and S. N. Black, *et al.*, *Acta Crystallogr., Sect. B: Struct. Sci.*, 2006, **62**, 498–505.